Photoelectron studies of neutral Ag_3 in helium droplets

Andreas Przystawik, Paul Radcliffe,[a] Thomas Diederich,[a] Tilo Döppner, Josef Tiggesbäumker, and Karl-Heinz Meiwes-Broer
Institut für Physik, Universität Rostock, 18051 Rostock, Germany

(Received 8 February 2007; accepted 14 March 2007; published online 11 May 2007)

Photoelectron spectra of neutral silver trimers, grown in ultracold helium nanodroplets, are recorded after ionization with laser pulses via a strong optical resonance of this species. Varying the photon energy reveals that direct vertical two-photon ionization is hindered by a rapid relaxation into the lower edge of a long-living excited state manifold. An analysis of the ionization threshold of the embedded trimer yields an ionization potential of 5.74±0.09 eV consistent with the value found in the gas phase. The asymmetrical form of the electron energy spectrum, which is broadened toward lower kinetic energies, is attributed to the influence of the matrix on the photoionization process. The lifetime of the excited state was measured in a two-color pump-probe experiment to be 5.7±0.6 ns. © *2007 American Institute of Physics*. [DOI: 10.1063/1.2723087]

I. INTRODUCTION

To date, predominantly negatively charged metal clusters have been investigated by *photoelectron spectroscopy* (PES). This technique probes the energy surfaces of the neutral in the geometry of the anion, which can differ significantly from the structure of the uncharged particle. A prominent example of such a geometry change was found in the charge reversal experiments on Ag_3^-, which indicate a subpicosecond, linear to triangular geometry change upon photodetachment.[1,2] To study neutrals with PES one must overcome two major obstacles, (i) selection of a *single* cluster size and (ii) the high *ionization potential* (IP), which lies in the vacuum ultraviolet region for most neutral species. By ionizing via a size-specific, long-living optically active state [*resonant two-photon ionization* (R2PI)], both mass selection and ionization can simultaneously be achieved for the silver trimer. The IP of free Ag_3 was determined by single photon laser ionization studies to be 5.73 eV.[3] Duncan and coworkers measured the vibronic spectrum of the $B\,^2E''$ state with the origin at 3.34 eV above the ground state.[4,5] The R2PI spectrum of *embedded* Ag_3, obtained by Federmann *et al.*,[6] shows a broad region of optical activity between 3.35 and 3.85 eV, which we refer to here as M^*. The position of M^* agrees well with the absorption spectrum of free Ag_3 derived from *ab initio* calculations.[7] The authors predict a C_{2v} ground state structure with strong transitions at energies of 3.41, 3.48, 3.71, and 3.75 eV. By selectively exciting Ag_3 via M^* details of the ionization dynamics are presented, taking the known IP of the free cluster as a reference.

Helium nanodroplets represent an ultracold and near perfect medium for spectroscopic studies at subkelvin temperatures, see Refs. 8–11 for details. In a molecular beam they have a large *pickup* cross section. It has recently been shown for magnesium that up to 2000 atoms could be loaded into a single droplet.[12] Helium droplets interact weakly with embedded neutral species. However, it is well known that a strong interplay between *charged* dopants and the surrounding helium exists.[13] As a consequence the photoionization process of an embedded particle should be influenced, e.g., the kinetic energy of the photoejected electrons might be altered in comparison to ionization in the gas phase. In a recent publication Loginov *et al.*[14] compared photoelectron spectra of free and in helium droplet dissolved molecules. They found a decrease of the IP of about 100 meV and a droplet size dependent asymmetric broadening of the structures in the spectra. It was suggested that the broadening is caused by inelastic collisions of the photoelectrons with the helium atoms of the droplet. Increased knowledge about the underlying dynamical processes after excitation and ionization will be important in successfully understanding the spectral identity of more complex systems, for example, large molecules, as well as metal clusters.

The paper is organized as follows. The experimental method for growing neutral silver clusters in helium droplets is briefly presented in Sec. II. Sections III A–III D contain the results and discussion on photoelectron spectroscopy of Ag_3 including the ionization dynamics and the lifetime of M^*. Section III C focuses on the influence of the helium environment on the photoemission process.

II. EXPERIMENTAL METHOD

The experimental technique of obtaining the photoelectron spectra of mass-selected neutral clusters in helium droplets via optical excited states [*resonant two-photon electron spectroscopy* (R2PES)] was already demonstrated for Ag_8 and Ag_2 (see Refs. 15 and 16). Helium droplets are generated in a supersonic nozzle source cooled by a liquid helium cryostat to 9–16 K.[17] The droplets are loaded with atoms from a metal vapor produced by a heated oven filled with silver. By varying the expansion conditions of the helium or the vapor density in the pickup region, the size distribution of the metal core can be influenced. Silver clusters with up to 150 atoms can grow inside the droplet.[18] The ultracold and

[a]Present address: HASYLAB at DESY, Notkestraße 85, 22607 Hamburg, Germany.

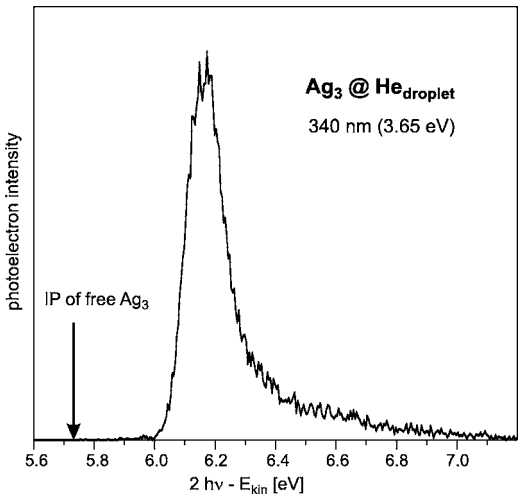

FIG. 1. Photoelectron spectrum of Ag_3 in He droplets after two-photon ionization at 340 nm. The known ionization potential of Ag_3 in the gas phase (5.73 eV) (Ref. 3) is shown for comparison. The explanation for the deviation from the measured threshold is given in the text.

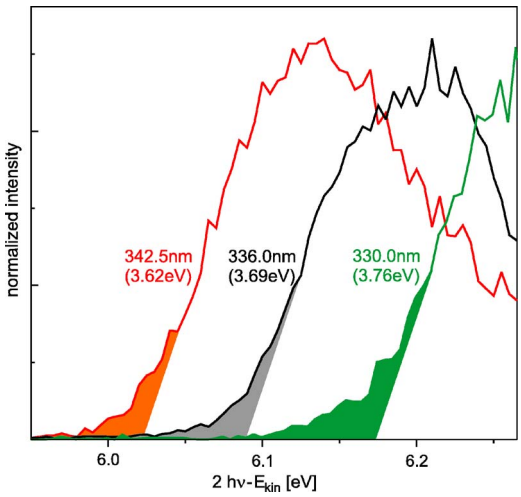

FIG. 2. Photoelectron spectra of Ag_3 in He droplets at three selected wavelengths. If a direct two-photon process were responsible for the ionization, no shift of the apparent binding energy $2h\nu - E_{kin}$ would be expected. The shaded areas under the curves visualize the washing out of the thresholds seen when exciting with higher photon energies.

chemically inert droplets transport the clusters into the ionization regions of a magnetic bottle-type photoelectron spectrometer and a high resolution reflectron time-of-flight mass spectrometer. Here, the cluster beam interacts with nanosecond light pulses from tunable laser systems. In order to enable the classification of the measured electron signals, the corresponding mass spectra are recorded. For the present investigations the source conditions are tuned in order to maximize the signal of Ag_3. The photoelectron spectrometer was calibrated by nonresonant multiphoton ionization of free magnesium atoms with electron energies in the range from 0.2 to 4.2 eV. From this measurement the instrumental resolution is determined to be approximately 30 meV at an electron kinetic energy of about 1 eV.

For the study of the excited state lifetime a two-color pump-probe setup is used. With two synchronized lasers, the second having approximately 1 eV higher photon energy, the two-color signal can be distinguished from the one-color signal in the electron time-of-flight spectrum.

III. RESULTS AND DISCUSSION

A. Spectroscopy of Ag_3

The optical spectrum of Ag_3 in helium droplets exhibits a strong resonance in the range from 3.35 up to 3.85 eV.[6] No other silver cluster shows a significant ionization cross section in that region. Hence excitation into M^* can be used to exclusively select Ag_3. The R2PE spectrum after excitation with 340 nm is shown in Fig. 1. We obtain a single peak with a threshold at significantly higher energy than the gas phase IP and asymmetrically broadened to higher binding energies. The full width at half maximum (FWHM) of the peak of about 150 meV is significantly larger than the resolution of the spectrometer itself. Finer vibronic structures, as measured in the gas phase by R2PI,[19] have meV separation, which is beyond the resolution of our present setup.

Neutral *single* photon electron spectroscopy maps the potential energy surface of the cation in the geometry of the neutral. Hence, the spectrum corresponds to a transition from Ag_3 into the cation Ag_3^+ ground state, $^2B_2 \leftarrow {}^1A_1$, which can be assigned to the IP of Ag_3. The vertical IP is known from gas phase experiments to be 5.73 eV.[3] The apparent disagreement between the experimental IPs might be due to a change of the geometry after excitation into M^*. The corresponding potential energy surfaces of the neutral have been calculated.[20] Due to Jahn-Teller interaction, the electronic ground state structure ($^2E'$ in D_{3h} symmetry) is distorted from an equilateral triangle into an obtuse triangle ($^2B_2$, C_{2v} symmetry). The global minimum lies 0.02 eV below the first excited state ($^2A_1$) and 0.15 eV below the linear transient $^2\Sigma_u^+$. The calculations suggest that the excited state geometry differs only slightly from the ground states of the neutral and the ion. Thus, no significant shift of the IP due to the two-photon ionization is expected. Therefore, the large difference suggests that other processes contribute when ionizing embedded trimers with R2PI.

B. Dynamics within M^*

The width of the excited state manifold M^* gives us an opportunity to study the wavelength dependence of the photoemission process and its possible dynamics. The measurements show an increase of the apparent electron binding energy $2h\nu - E_{kin}$ with increasing photon energy (see Fig. 2). In addition the ionization threshold flank becomes shallower. In order to analyze the threshold kinetic energy E_{kin} (here we take the crossing of a tangent at the steepest point of the low energy flank with the energy axis), it is plotted versus the corresponding photon energy E_p (see Fig. 3). In the simplest case E_{kin} should follow a linear dependence.

$$E_{kin} = NE_p - \Delta E, \tag{1}$$

where ΔE is the energy difference to the vacuum potential. The corresponding fit through the data points determines the number of absorbed photons N and ΔE. For a vertical two-photon process one would expect $N=2$ with ΔE equal

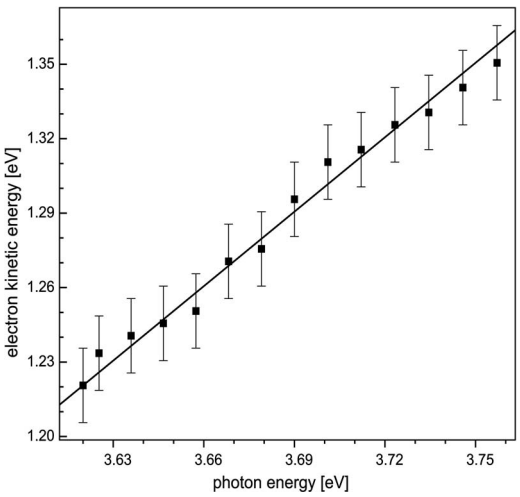

FIG. 3. Kinetic energy of the threshold photoelectrons as a function of the photon energy. The slope of the fit [Eq. (1)] indicates that a rapid relaxation occurs before the absorption of the second photon. The ionization proceeds from a fixed level of Ag_3 located 2.40 ± 0.09 eV below the IP.

to the IP. However, the fit gives a slope of virtually 1 ($N=0.95\pm0.05$); hence the ionization takes place from an excited state independent of the photon energy used to promote Ag_3 into M^*. Thus any excess energy is dissipated before the second photon couples into the cluster. From the fit a value of

$$\Delta E = 2.40 \pm 0.09 \text{ eV} \tag{2}$$

below the ionization threshold is obtained. This indicates a rapid relaxation of Ag_3 to the lower edge of M^* located 2.4 eV below the ionic ground state energy before the absorption of the second photon. The ionization starts from this particular level, irrespective of the excitation energy.

Further insight to the excited state dynamics can be gained from the change of the photoelectron signal close to the threshold. When a higher photon energy is used for excitation, the low-energy tails marked in Fig. 2 increase in length, indicating that at least a part of the signal results from trimers with some excess energy left. That hints to a stepwise thermalization process and the overall relaxation time depends on the chosen excitation energy. Since the laser pulse has a width of 6 ns (FWHM), the relaxation process must proceed on a comparable but shorter time scale. A value of several hundreds of picoseconds is feasible. Otherwise one would expect that a significant fraction of not fully relaxed trimers contribute to the signal leading to an even larger broadening of the photoelectron spectra in the threshold region.

A fast relaxation toward thermal equilibrium is typical for species embedded in matrices. Recently it was shown that aniline molecules as well as Ag_8 clusters embedded in helium droplets exhibit a relaxation upon electronic excitation on the picosecond time scale.[14,15] Furthermore, rotationally resolved spectra of tetracene and pentacene in helium droplets show a lifetime broadening due to vibrational relaxation in the range of 1 ps.[21] In addition, energy could be directly coupled into the surrounding helium at excitation. The influence on the electronic transitions of atoms can be understood in the frame of a bubble model.[22,23] Due to the different shapes and extensions of the electron wave functions of the involved states, one excites a broad band of bubble oscillations (*ripplon* states). The bubble relaxes within picoseconds to its equilibrium geometry, thus dissipating the energy to the helium matrix. The existence of this effect upon excitation of molecules and small clusters is also conceivable.

Independent of the mechanism, the system undergoes a rapid relaxation to the lower edge of M^*. This level can be identified with the band origin of the $B\,^2E''$ state which has been measured in the gas phase by Cheng and Duncan at an energy of 3.34 eV.[4] Also fluorescence from Ag trimers embedded in an argon matrix is observed in the same energy range (3.32 eV).[24] It is therefore highly probable that in all three experiments the same $B\,^2E''$ state is probed. Assuming a complete relaxation of Ag_3 within the $B\,^2E''$ state and neglecting any influence of the helium environment on the measured threshold energy of the photoelectrons yield an IP of $3.34+2.40=5.74\pm0.09$ eV in excellent agreement with the one-photon IP of 5.73 eV measured in the gas phase.[3]

C. Influence of the helium environment on the photoemission process

Despite the fact that virtual identical values for the IP of Ag_3 in helium droplets and in the gas phase were found, the electron emission process is influenced by the presence of the surrounding helium. This may affect the final kinetic energy of the individual emitted electrons hence broadening and potentially shifting the photoelectron spectrum of the embedded Ag_3. The dominant short range electron-helium interaction is strongly repulsive, making a barrier of about 1.0 eV for electrons entering the liquid surface. The bubble formed around an electron in helium is as large as 3.4 nm.[25] The initial formation time is thought to be in the range of a few picoseconds[25,26] with thermalization finished after 150 ps.[27] However, in helium *droplets* under the present experimental conditions, an electron will have left the droplet after about 10 fs, much less than the bubble formation time. Hence, the electron upon leaving causes probably just a small perturbation to the droplet and is emitted losing only a fraction of its energy. The observed asymmetric broadening of the photoelectron spectra could indicate such a process. In a first approach elastic binary collisions of the photoelectrons with individual helium atoms might be considered to be responsible for the observed shape. Loginov *et al.* suggested a convolution of a Gaussian and an exponential decay as an empirical fit to the spectra.[14] They interpreted the linear dependence of the exponential decay constants from the droplet size as evidence for the validity of the approach. Such a fit to the spectrum in Fig. 1 yields an exponential decay constant of 68 ± 3 meV at an average droplet radius of 55 Å, which matches the values published in Ref. 14. However, as clearly seen in Fig. 1, a significant part of the photoelectron signal spreads over an energy range of about 500 meV. The fit does not account for this long tail of slower electrons. Still, it cannot be excluded that the tail is a feature of the system itself. To the best of our knowledge no gas phase photoelec-

tron spectra of neutral Ag_3 have been published. Therefore, we compare the measured profile to work on the anions, which are linear in the ground state.[28,29] These spectra show much narrower peaks. Asymmetric broadening is also evident, but appears on the low binding energy wing of the peak. The authors attribute the broadening to $\tilde{X}\,^2B_2 \leftarrow \tilde{X}\,^1\Sigma_g^+$ transitions from higher vibrational levels of the linear molecule into excited vibrational states of the neutral triangular trimer. No evidence of a prominent tail structure to higher binding energy was observed (see Fig. 7 of Ref. 28). It is known that the ionization process causes no significant change in the cluster geometry, whereas the electron detachment process induces a linear-triangular transition of the trimer. Therefore, it is probable that the long tail of low energy electrons does not reflect the density of states in the Ag_3 ion. Thus a more sophisticated model is needed to describe the electron-helium scattering and possible inelastic processes.

Loginov *et al.* have found a droplet size dependent lowering of the ionization potential of aniline molecules in helium in the range of 100 meV.[14] They were able to describe the dependence in the frame of the polarizable continuum model.[30,31] The ionization potential of the system under study should be related to the droplet radius R as

$$\mathrm{IP}(R) = \mathrm{IP}_\infty + \frac{e^2(1-\varepsilon^{-1})}{8\pi\varepsilon_0 R}, \tag{3}$$

where IP_∞ is the ionization potential in bulk helium, e the electron charge, and ε the dielectric constant of the helium droplet. However, we note that this simple equation is only able to correctly describe the asymptotic behavior of larger droplets. The absolute shift of the IP, i.e., the difference of IP_∞ to the gas phase value, is strongly dependent on the microscopic structure around the embedded species and the short range interactions between the solute and the helium. It is vastly different when comparing, e.g., an aniline molecule with Ag_3. Most molecules show comparatively strong attractive interactions and an increased helium density around the molecule, whereas single atoms and small atomic clusters are more loosely bound to the droplet and often form a small bubble with a reduced helium density, especially when electronically excited. This leads to a much smaller difference between IP_∞ and the gas phase value. Therefore, we conclude that the photoelectron *threshold* of Ag_3 in a helium droplet matches the ionization potential of the free species within the resolution of our experimental setup, whereas the overall *shape* is significantly affected by the presence of the helium nanodroplet environment.

D. Lifetime of the $B\,^2E''$ state

Finally we address the relaxation dynamics of the $B\,^2E''$ state. Since this state can be probed by single nanosecond laser pulses one is able to investigate the lifetime by applying the pump-probe technique without using ultrafast laser systems. The first laser pulse at 342 nm (3.63 eV) prepares Ag_3 in the excited state manifold M^* which quickly relaxes down to the $B\,^2E''$ state. After a certain delay the second laser pulse probes the remaining population in that state. From the time evolution of the pump-probe signal the lifetime can be

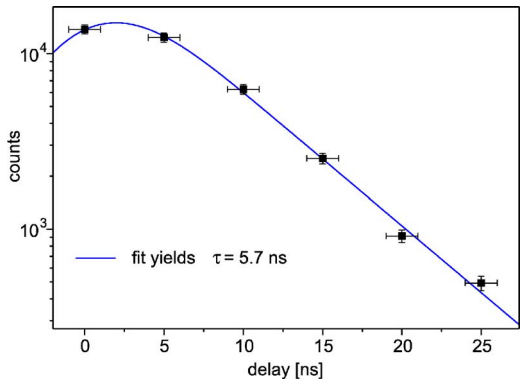

FIG. 4. Two-color pump-probe signal of the $B\,^2E''$ level. The data are fitted by an exponential decay convoluted with a Gaussian which accounts for the finite width of the laser pulses (6 ns FWHM). The fit gives an excited state lifetime of 5.7±0.6 ns.

determined. Furthermore, pump-probe photoelectron spectra may reveal the existence of lower lying levels into which the excited Ag_3 might relax. The dynamics is probed by recording the photoelectron spectra as a function of the delay between the two laser pulses. In order to be able to uniquely assign the electron signal to the pump and the probe pulse, a different photon energy for the second laser pulse was chosen in the experiment. The electrons originating from ionization with the probe pulse form a duplicated spectrum shifted by the difference of the photon energies. In the measurement presented here, the fourth harmonic of a neodymium doped yttrium aluminum garnet laser with a wavelength of $\lambda = 266$ nm (4.66 eV) was used as the probe pulse. The pump-probe signal results in the appearance of an additional peak at approximately 1 eV higher kinetic energies. Tuning the pump-probe separation toward larger delay times, the intensity of this peak decreases indicating a delay of the $B\,^2E''$ state.

Figure 4 shows the pump-probe signal as a function of the delay between the pulses. The widths of the laser pulses (6 ns FWHM) are comparable to the lifetime itself. Here, the data points are fitted to an exponential decay curve convoluted with the Gaussian shape of the laser pulses. Taking into account a possible jitter of the electronic synchronization of the two pulses, the excited state has a lifetime of $\tau = 5.7 \pm 0.6$ ns. With the chosen probe wavelength no additional structure appears at lower electron kinetic energies. Thus the final state after relaxation is bound by more than 4.6 eV. Considering the measured lifetime, it is probable that Ag_3 decays to the ground state by fluorescence. However, experiments are under way to identify a possible relaxation to lower lying excited states by applying higher probe photon energies, for example, with anti-Stokes lines from a H_2-Raman cell. This may reveal competitive decay processes, i.e., internal conversion, intersystem crossing, or predissociation. For a triatomic molecule such as Ag_3 irreversible nonradiative decay is unlikely because the density of vibronic states is too low. However, coupling of the initially excited state to other electronic states, which themselves show broadened energy levels due to predissociation, may allow such a decay. Thus, a sequential model leading to predissociation is also conceivable. The trimer is known to dis-

sociate when excited in the droplets.[6] If the helium environment is efficient enough in dissipating the excess energy, it may be possible for the excited-state system to relax back to the ground state in a nonradiative way, though experimental evidence is lacking.

IV. CONCLUSION

In conclusion, information about the electronic structure of neutral Ag_3 in helium nanodroplets was obtained by combining resonant two-photon ionization and photoelectron spectroscopy. The optical excitation is used to select Ag_3 from the cluster size distribution present in the droplet beam. A rapid decay on a subnanosecond time scale down to the longer living $B\,^2E''$ state known from gas phase spectroscopy is observed. The excess energy is effectively dissipated in the helium environment. Taking this process into account, the value found for the ionization potential of the embedded trimer is in accordance with results from one-photon ionization experiments on gas phase Ag_3. The influence of the helium environment on the photoemission threshold is negligible but the shape of the photoelectron signal, especially the low energy tail, results from the interaction with the surrounding environment. Using a two-color excitation scheme the lifetime of the $B\,^2E''$ state was measured and a value of 5.7 ns was obtained. The experiments show that R2PES is a powerful tool to probe molecules and clusters embedded in helium droplets.

ACKNOWLEDGMENTS

The authors gratefully acknowledge financial support by the Deutsche Forschungsgemeinschaft through Sonderforschungsbereich 652 and the Graduiertenkolleg 567. They thank Professor Toennies and his group, who designed and constructed main parts of the helium droplet machine.

[1] S. Wolf, G. Sommerer, S. Rutz, E. Schreiber, T. Leisner, L. Wöste, and R. S. Berry, Phys. Rev. Lett. **74**, 4177 (1995).
[2] D. Boo, Y. Ozaki, L. Anderson, and W. Lineberger, J. Phys. Chem. **101**, 6688 (1997).
[3] G. Alameddin, J. Hunter, D. Cameron, and M. Kappes, Chem. Phys. Lett. **192**, 122 (1992).
[4] P. Cheng and M. Duncan, Chem. Phys. Lett. **152**, 341 (1988).
[5] K. LaiHing, P. Cheng, and M. Duncan, Z. Phys. D: At., Mol. Clusters **13**, 161 (1989).
[6] F. Federmann, K. Hoffmann, N. Quaas, and J. Toennies, Eur. Phys. J. D **9**, 11 (1999).
[7] V. Bonačić-Koutecký, J. Pittner, M. Boiron, and P. Fantucci, J. Chem. Phys. **110**, 3876 (1999).
[8] M. Hartmann, R. Miller, J. Toennies, and A. Vilesoy, Phys. Rev. Lett. **75**, 1566 (1995).
[9] Special issue on He droplets, J. Chem. Phys. **115** (2001).
[10] A. Scheidemann, B. Schilling, and J. Toennies, J. Phys. Chem. **97**, 2128 (1993).
[11] S. Goyal, D. Schutt, and G. Scoles, Phys. Rev. Lett. **69**, 933 (1992).
[12] T. Diederich, T. Döppner, T. Fennel, J. Tiggesbäumker, and K.-H. Meiwes-Broer, Phys. Rev. A **72**, 023203 (2005).
[13] K. A. Atkins, Phys. Rev. **116**, 1339 (1959).
[14] E. Loginov, D. Rossi, and M. Drabbels, Phys. Rev. Lett. **95**, 163401 (2005).
[15] P. Radcliffe, A. Przystawik, T. Diederich, T. Döppner, J. Tiggesbäumker, and K.-H. Meiwes-Broer, Phys. Rev. Lett. **92**, 173403 (2004).
[16] A. Przystawik, P. Radcliffe, S. Göde, K.-H. Meiwes-Broer, and J. Tiggesbäumker, J. Phys. B **39**, S1183 (2006).
[17] A. Bartelt, J. Close, F. Federmann, N. Quaas, and J. Toennies, Phys. Rev. Lett. **77**, 3525 (1996).
[18] T. Diederich, J. Tiggesbäumker, and K.-H. Meiwes-Broer, J. Chem. Phys. **116**, 3263 (2002).
[19] F. Wallimann, H. Frey, S. Leutwyler, and M. Riley, Z. Phys. D: At., Mol. Clusters **40**, 30 (1997).
[20] M. Hartmann, J. Pittner, V. Bonačić-Koutecký, A. Heidenreich, and J. Jortner, J. Chem. Phys. **108**, 3096 (1998).
[21] M. Hartmann, A. Lindinger, J. Toennies, and A. Vilesov, J. Phys. Chem. A **105**, 6369 (2001).
[22] J. Jakubek, Q. Hui, and M. Takami, Phys. Rev. Lett. **79**, 629 (1997).
[23] J. Reho, U. Merker, M. Radcliff, K. Lehmann, and G. Scoles, J. Chem. Phys. **112**, 8409 (2000).
[24] S. Fedrigo, W. Harbich, and J. Buttet, J. Chem. Phys. **99**, 5712 (1993).
[25] M. Rosenblit and J. Jortner, Phys. Rev. Lett. **75**, 4079 (1995).
[26] D. Onn and M. Silver, Phys. Rev. A **3**, 1773 (1971).
[27] A. Benderskii, J. Eloranta, R. Zadoyan, and V. Apkarian, J. Chem. Phys. **117**, 1201 (2002).
[28] J. Ho, K. Ervin, and W. Lineberger, J. Chem. Phys. **93**, 6987 (1990).
[29] H. Handschuh, C. Cha, P. Bechthold, G. Ganteför, and W. Eberhardt, J. Chem. Phys. **102**, 6406 (1995).
[30] J. Jortner, Z. Phys. D: At., Mol. Clusters **24**, 247 (1992).
[31] G. Makov and A. Nitzan, J. Phys. Chem. **98**, 3459 (1994).